

## Small membranes under negative surface tension

Yotam Y. Avital and Oded Farago

Citation: *The Journal of Chemical Physics* **142**, 124902 (2015); doi: 10.1063/1.4915512

View online: <http://dx.doi.org/10.1063/1.4915512>

View Table of Contents: <http://scitation.aip.org/content/aip/journal/jcp/142/12?ver=pdfcov>

Published by the [AIP Publishing](#)

---

### Articles you may be interested in

[Tension moderation and fluctuation spectrum in simulated lipid membranes under an applied electric potential](#)

*J. Chem. Phys.* **139**, 164902 (2013); 10.1063/1.4826462

[Thermal fluctuations and bending rigidity of bilayer membranes](#)

*J. Chem. Phys.* **139**, 094902 (2013); 10.1063/1.4818421

[Coarse-grained simulations of membranes under tension](#)

*J. Chem. Phys.* **132**, 115101 (2010); 10.1063/1.3352583

[Simulations of edge behavior in a mixed-lipid bilayer: Fluctuation analysis](#)

*J. Chem. Phys.* **126**, 045105 (2007); 10.1063/1.2430714

[Statistical mechanics of bilayer membrane with a fixed projected area](#)

*J. Chem. Phys.* **120**, 2934 (2004); 10.1063/1.1639000

---



## Small membranes under negative surface tension

Yotam Y. Avital and Oded Farago

*Department of Biomedical Engineering and Ilse Katz Institute for Nanoscale Science and Technology, Ben-Gurion University of the Negev, Be'er Sheva 84105, Israel*

(Received 5 January 2015; accepted 9 March 2015; published online 26 March 2015)

We use computer simulations and a simple free energy model to study the response of a bilayer membrane to the application of a negative (compressive) mechanical tension. Such a tension destabilizes the long wavelength undulation modes of giant vesicles, but it can be sustained when small membranes and vesicles are considered. Our negative tension simulation results reveal two regimes—(i) a weak negative tension regime characterized by stretching-dominated elasticity and (ii) a strong negative tension regime featuring bending-dominated elastic behavior. This resembles the findings of the classic Evans and Rawicz micropipette aspiration experiment in giant unilamellar vesicles (GUVs) [E. Evans and W. Rawicz, *Phys. Rev. Lett.* **64**, 2094 (1990)]. However, in GUVs the crossover between the two elasticity regimes occurs at a small positive surface tension, while in smaller membranes it takes place at a moderate negative tension. Another interesting observation concerning the response of a small membrane to negative surface tension is related to the relationship between the mechanical and fluctuation tensions, which are equal to each other for non-negative values. When the tension decreases to negative values, the fluctuation tension  $\gamma$  drops somewhat faster than the mechanical tension  $\tau$  in the small negative tension regime, before it saturates (and becomes larger than  $\tau$ ) for large negative tensions. The bending modulus exhibits an “opposite” trend. It remains almost unchanged in the stretching-dominated elastic regime, and decreases in the bending-dominated regime. Both the amplitudes of the thermal height undulations and the projected area variations diverge at the onset of mechanical instability. © 2015 AIP Publishing LLC. [<http://dx.doi.org/10.1063/1.4915512>]

### I. INTRODUCTION

Bilayer membranes are quasi-two-dimensional (2D) fluid sheets formed by spontaneous self-assembly of lipid molecules in water.<sup>1</sup> Their elasticity is traditionally studied in the framework of the Helfrich effective surface Hamiltonian for 2D manifolds with local principle curvatures  $c_1$  and  $c_2$ ,<sup>2</sup>

$$\mathcal{H} = \int_A dS \left[ \sigma_0 + \frac{1}{2} \kappa_0 (c_1 + c_2 - 2c_0)^2 + \bar{\kappa}_0 c_1 c_2 \right], \quad (1)$$

where the integration is carried over the whole surface of the membrane. The Helfrich Hamiltonian involves four parameters: the spontaneous curvature  $c_0$ , the surface tension  $\sigma_0$ , the bending modulus  $\kappa_0$ , and the saddle-splay modulus  $\bar{\kappa}_0$ . For symmetric bilayer membranes,  $c_0 = 0$ . If, in addition, the discussion is limited to deformations that preserve the topology of the membrane, then (by virtue of the Gauss-Bonnet theorem) the total energy associated with the last term is constant, and one arrives to the more simple form

$$\mathcal{H} = \int_A dS \left[ \sigma_0 + \frac{1}{2} \kappa_0 (c_1 + c_2)^2 \right] = \sigma_0 A + \frac{1}{2} \kappa_0 J^2, \quad (2)$$

where  $A$  is the total area of the membrane and  $J$ , defined by  $J^2 = \int dS (c_1 + c_2)^2$ , is the integrated squared total curvature.

Helfrich Hamiltonian provides successful framework for describing many features of bilayer membranes and vesicles, including their large-scale shapes and transformations between them,<sup>3</sup> membrane-membrane interactions,<sup>4</sup> and membrane-mediated forces between proteins (“inclusions”).<sup>5</sup> Yet, despite

of the success and the wide acceptance of the model, the surface tension term  $\sigma_0$  in Eq. (2) remains confusing and poorly understood. Below, we briefly review some of the complications associated with the concept of membrane surface tension.

1. Membranes are much more flexible to bending than stretching. Therefore, in theoretical studies, it is sometimes assumed that the lipids area density is fixed<sup>6</sup> and changes in the total area result in from changes in the number of lipids.<sup>7</sup> In this picture, the surface tension is essentially the chemical potential of the surface lipids.<sup>8</sup> Lipids, however, are highly insoluble in water (their critical micelle concentration is typically in the  $<10^{-6}\text{M}$  range<sup>1</sup>), which makes the above interpretation for the surface tension largely irrelevant as there is almost no exchange of lipids between the bilayer membrane and the embedding aqueous medium. More commonly, the surface tension is considered as a measure for the elastic response of a membrane with a fixed number of lipids to area variations.<sup>9,10</sup> This view clearly differs from the meaning of the term “surface tension” for fluid/fluid interfaces, where it serves as a measure for the free energy penalty resulting from an exchange of molecules between the “bulk” phases and the “interface.”<sup>11</sup>

2. Further complication arises from the fact that the membrane is a (quasi) two dimension manifold embedded in a three dimensional space. Therefore, it has two characteristic areas—(i) the total physical area,  $A$ , and (ii) the area of its projection onto a planar reference frame,  $A_p$ . Helfrich Hamiltonian involves an integral over the total area  $A$ ; but this area (whose determination, taking into account the molecular structure of the membrane, is not without ambiguity) cannot

be fixed due to the membrane thermal undulations. Thus,  $A$  is not a valid thermodynamic variable.<sup>12</sup> It is, in fact, the projected area  $A_p$  that emerges as the computationally relevant quantity.<sup>13</sup> The force per unit length that needs to be imposed on the frame in order to fix its area to  $A_p$  is known as the *mechanical (frame) tension*, and will be denoted henceforth by  $\tau$ . Theoretically, the mechanical tension can be identified with the derivative of the elastic free energy,  $F$ , with respect to  $A_p$ :  $\tau = \partial F / \partial A_p$  (where the differentiation is carried while holding the volume of the system, as well as the temperature and number of lipids, fixed). One can also fix  $\tau$  and let  $A_p$  fluctuate. In this case, the relevant free energy is  $G = F - \tau A_p$  and the mean projected area satisfies  $\langle A_p \rangle = -\partial G / \partial \tau$ .

3. Another confusing aspect associated with the concept of surface tension is the distinction between Helfrich Hamiltonian and the membrane free energy  $F$ . The latter is often referred to as the *Helfrich free energy*, and the confusion arises because it is assumed to have the same form as the Helfrich Hamiltonian,

$$F = \sigma \bar{A} + \frac{1}{2} \kappa \bar{J}^2. \quad (3)$$

In Equation (3),  $\bar{A}$  and  $\bar{J}$  denote, respectively, the area and squared total curvature of the *mean profile* of the membrane. Eq. (3) features two *renormalized* coefficients, the tension  $\sigma$  and bending modulus  $\kappa$ , that are not equal to their *intrinsic* counterparts from Eq. (2),  $\sigma_0$  and  $\kappa_0$ . The statistical mechanics of thermal fluctuations around the mean profile are accounted for in the values of the renormalized elastic coefficients. For a membrane with a mean flat profile (i.e., not subjected to normal bending forces),  $\bar{A} = A_p$  and  $\bar{J} = 0$ . Then, Eq. (3) takes the form  $F = \sigma A_p$  and  $\tau = \partial F / \partial A_p = \sigma$ .

4. Another quantity that can be identified as the membrane surface tension is the, so called,  $q^2$ -coefficient  $\gamma$ , also known as the *fluctuation tension*. The fluctuation tension is measured from the Fourier spectrum of the membrane height function with respect to the plane of the frame. For a membrane with a mean flat profile, the thermal average of the amplitude of a Fourier mode with wavevector  $\vec{q}$  satisfies:  $\langle h_{\vec{q}} \rangle = 0$  and

$$\langle |h_{\vec{q}}|^2 \rangle = \frac{k_B T A_p}{l^4 [\gamma q^2 + \kappa q^4 + O(q^6)]}, \quad (4)$$

where  $k_B$  is Boltzmann constant,  $T$  is the temperature, and  $l$  is a microscopic cutoff length. Some controversy surrounded Eq. (4) concerning the question whether  $\gamma$ , the  $q^2$ -coefficient in the denominator on the right hand side, is equal to  $\sigma_0$  or  $\sigma$ . This issue has been recently settled, and it is now understood that the correct coefficient is the renormalized surface tension  $\sigma$ ,<sup>14,15</sup> or, according to some theoretical studies, a slightly modified version of this surface tension,  $(A_p/A)\sigma$ .<sup>16</sup> Similarly, the  $q^4$  coefficient in Eq. (4) is equal to the renormalized bending modulus  $\kappa$ . Combining this with the discussion about Eq. (3), we conclude that both the measurable fluctuation and mechanical tensions coincide with each other (and with the renormalized tension  $\sigma$ ):  $\gamma = \tau = \sigma$ .

## II. NEGATIVE SURFACE TENSION

When the surface tension  $\tau = \gamma = \sigma$  vanishes, the membrane is “free to choose” the equilibrium projected area  $A_p$  that minimizes the free energy  $G = F$ . The question we now wish to address concerns with the elastic response of the membrane to a further decrease in the frame area, which involves the application of a negative surface tension. Based on Eq. (4), one may argue that for  $\gamma < 0$ , the membrane always becomes mechanically unstable because the amplitude of any mode with  $q < \sqrt{-\gamma/\kappa}$  diverges. But such modes exist only in sufficiently large membranes, hence, small membranes can always sustain some negative surface tension. For instance, consider a square membrane of linear size  $L$  with  $\kappa = 25k_B T \approx 10^{-19}$  J. From Eq. (4), one finds that such a membrane can withstand negative surface tension of size  $\gamma = -5 \times 10^{-3}$  N/m (which is comparable in magnitude to the typical positive rupture tension), provided that  $L < (2\pi)\sqrt{-\kappa/\gamma} \sim 30$  nm. This is the characteristic size of real small liposomes and of bilayers in highly coarse-grained simulations. Thus, the above estimation highlights the fact that the question of elastic response to negative surface tension is both interesting and relevant to current experimental and computational studies.

The derivation of Eq. (4), and the proof that the fluctuation and mechanical tensions coincide with each other, involves several assumptions that do not necessarily remain valid when  $\sigma$  becomes negative. Specifically, it is based on the investigation of the linear response of a mechanically *stable* flat membrane to small normal forces and is restricted to configurations with smooth (twice differentiable) height functions  $h(\vec{r})$ . But when  $\sigma < 0$ , the membrane can relieve the free energy cost of compression by buckling. We note that *in the absence of normal forces* (which is the case under consideration here), the system is not expected to undergo spontaneous symmetry breaking similar to that occurring, e.g., in Ising spin systems below the critical point. The reason is that the membrane height profile  $h(\vec{r})$  is a continuous field and, therefore, the transition between different buckled configurations (e.g., from buckled “upward” to “downward”) does not require the crossing of a free energy barrier. Thus, the system remains ergodic for negative tension, and due to the symmetry of the bilayer,  $\langle h_{\vec{q}} \rangle = 0$  for all the Fourier modes. The questions that remain are as follows.

1. Does Eq. (4) still hold for  $\sigma < 0$ ? We certainly do not expect it to remain valid for strongly compressed membranes since it is derived from a quadratic (in the height function) approximation to full Helfrich Hamiltonian (2). However, considering the fact that it holds for  $\sigma = 0$ , there is no apparent reason why it should not hold for small negative  $\sigma$ .

2. Are the mechanical and fluctuation tensions still equal to each other? (Obviously, this question is relevant only if the answer to question no. 1 is “yes.”) As noted above, the proof of this equality depends on the surface tension being positive. Now that it is negative, the membrane prefers more buckled configurations with larger mean squared amplitudes. Does this imply that the fluctuation tension  $\gamma$  drops faster (i.e., becomes more negative) than the mechanical tension  $\tau$ ?

3. What happens to the bending modulus  $\kappa$  under compression? Recall that the coefficient appearing in Eq. (4) is the

renormalized bending modulus which, just like the tension  $\gamma$ , may vary with the frame area  $A_p$ . For positive tensions, the variations in  $\kappa$  are usually negligible, but this may not be the case for negative tensions when the membrane becomes increasingly more buckled. Does the increase in the degree of buckling under larger compressive stresses involve a decrease in  $\kappa$ ?

4. Does the membrane exhibit linear (Hookean) elastic response to negative mechanical tension? In response to a positive tension, the membrane becomes stretched and the relationship between the change in the area (strain) and the stress is indeed linear. However, the lipids constitute a dense two-dimensional fluid and, therefore, the membrane can be barely compressed below its most favorable physical area  $A_0$ . When, under the application of a negative tension, the physical area  $A$  reaches  $A_0$ , the negative tension causes the membrane to buckle and more and more area is “stored” in the out-of-plane fluctuations. This could lead to a highly non-linear elastic response.

In what follows, we will use Monte Carlo (MC) simulations to address the above questions.

### III. COMPUTER SIMULATION METHODS

To allow for large scale membrane simulations ( $N = 1000$  lipids per monolayer) in a computationally feasible manner, we employ the Cooke-Deserno model,<sup>17</sup> with model parameters used in our recent work on fluid charged membranes.<sup>18</sup> In this highly coarse-grained model, the lipids are represented as trimers with one hydrophilic and two hydrophobic beads and the embedding solvent is handled implicitly via effective interactions between the hydrophobic beads. The membranes are simulated in a box of linear size  $L_x = L_y = L$ , with periodic boundary conditions in the  $x - y$  (frame) plane. Initially, we place a pre-assembled flat membrane at the center of the simulation box, and we then allow it to equilibrate for  $1 \times 10^5$  MC time units. On average, each MC time unit consists of  $N$  translation (with additional small intramolecular displacements) and  $N$  rotation move attempts carried on randomly chosen lipids. The membrane is simulated at constant frame tension  $\tau$ , which is accomplished by incorporating several move attempts, per time unit, to change the frame area of the membrane.<sup>19</sup> Each time unit also includes several collective “mode excitation” moves<sup>20</sup> that accelerate the slow dynamics of the long-wavelength Fourier modes. For each value of  $\tau$ , the initial thermalization period is followed by a period of  $1.5 \times 10^6$  MC time units during which we sample quantities of interest at 200 MC units intervals.

In what follows, we set the thermal energy  $k_B T$  to be the elementary energy unit and the length parameter of the Deserno-Cooke repulsive potential  $b$  to be the length unit. We simulate the membrane under frame tensions satisfying  $-0.3 \leq \tau \leq 0.5$  (in  $k_B T/b^2$  units) which, as revealed by our computational observations, is the stability range of the simulated membranes. Relation to physical units can be made by setting  $b = 0.65$  nm, which gives the unit of the surface tension  $k_B T/b^2 \simeq 10$  mN/m. For  $\tau > 0.5$ , the membranes rupture, while for  $\tau < -0.3$ , they exhibit large normal undulations lead-

ing to collapse and dissociation of lipids. Within the stability range, we measure the mean and variance of the projected area distribution ( $\langle A_p \rangle$  and  $\langle \delta A_p^2 \rangle = \langle A_p^2 \rangle - \langle A_p \rangle^2$ , respectively). We also calculate the Fourier transform of the height undulations, by dividing the membrane into  $8 \times 8$  grid cells and calculating the local mean height of the bilayer within each grid cell. The Fourier transform of  $h(\vec{r})$  in wavenumber space  $\vec{n} = \vec{q}(L/2\pi)$  ( $\vec{n} = (n_x, n_y)$ ;  $n_x, n_y = -4, -3, \dots, 2, 3$ ) is defined by

$$\tilde{h}_{\vec{n}} = \frac{1}{L} \sum_{\vec{r}} h(\vec{r}) e^{-2\pi i \vec{n} \cdot \vec{r} / L}. \quad (5)$$

Notice that the linear size of the frame  $L$ , appearing (twice) in the definition of  $h_{\vec{n}}$ , is not constant, but rather fluctuates during the course of the (constant tension) simulations. At each measurement, we use the instantaneous value of  $L$ . Also notice that  $h_{\vec{n}}$  defined in Eq. (5) is dimensionless, due to the  $L^{-1}$  prefactor that does not exist in the more commonly used  $h_{\vec{q}}$  of Eq. (4). In terms of the variable  $h_{\vec{n}}$ , Eq. (4) takes the form

$$\langle |h_{\vec{n}}|^2 \rangle = \left( \frac{L}{l} \right)^4 \frac{k_B T}{[\gamma \langle A_p \rangle (2\pi n)^2 + \kappa (2\pi n)^4]}. \quad (6)$$

There are four different modes corresponding to each value of  $|\vec{n}|$ , and this number is reduced to two if  $|n_x| = |n_y|$  or if one of the components of  $\vec{n}$  is zero. In Sec. IV, the results for  $\langle |h_{\vec{n}}|^2 \rangle$  (and other related quantities) represent averages over these distinct modes. In Eq. (6),  $l$  is the grid size, which implies that  $L/l = 8$ , independently of the instantaneous value of  $L$ .

Due to molecular-scale protrusion, the physical area of the membrane cannot be unambiguously determined. Therefore, we use the following approximation for  $\langle A \rangle$ :

$$\langle A \rangle \simeq \langle A_p \rangle \left[ 1 + \frac{1}{2} \left( \frac{l}{L} \right)^4 \sum_{\vec{n}} (2\pi n)^2 \langle |h_{\vec{n}}|^2 \rangle \right], \quad (7)$$

which is the physical area “visible” up to the resolution of the grid. One can also define the effective area-stretch modulus of the membrane,  $K_A$ , by assuming that the free energy cost due to small variations in the projected area from  $\langle A_p \rangle$  can be approximated by the quadratic form  $(1/2) K_A [A_p - \langle A_p \rangle]^2 / \langle A_p \rangle$ .<sup>8</sup> Under this approximation, the coefficient  $K_A$  can be extracted from the fluctuation statistics of  $A_p$  by using the equipartition theorem

$$K_A = \frac{k_B T \langle A_p \rangle}{\langle \delta A_p^2 \rangle}. \quad (8)$$

### IV. RESULTS

In Sec. II, we raised several questions concerning the elastic and fluctuation behavior of membranes under negative mechanical tension. Here, we present computer simulation results addressing those questions.

We begin with the question of the validity of Eq. (6) for negative frame tensions. Figure 1 displays our results for the fluctuation spectral intensity,  $|h_{\vec{n}}|^2$ , as a function of  $n^2$  for membranes under three different mechanical tensions  $\tau = -0.24, 0$ , and  $0.24$ . The fits of the computational results to Eq. (6)

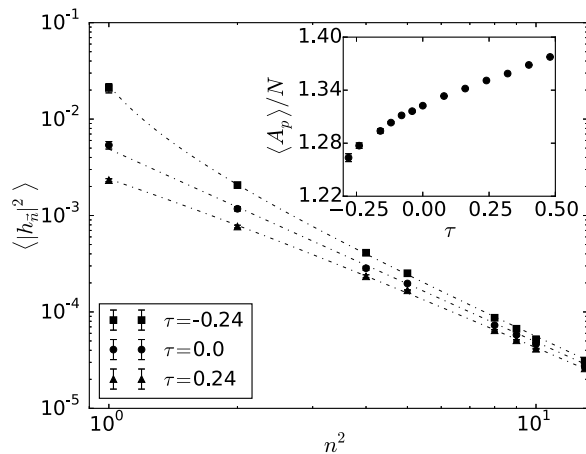


FIG. 1. The spectral intensity as a function of the wavenumber for membranes under frame tension of  $\tau = -0.24$  (squares), 0 (circles), and 0.24 (triangles). The dotted-dashed curves represent the best fits of the results to Eq. (6) over the first four modes. The inset shows the mean projected area per lipid as a function of  $\tau$ .

are displayed with dotted-dashed lines. Our analysis reveals that within most of the range of mechanical stability  $-0.3 \leq \tau \leq 0.5$ , the quality of each fit is very good. This demonstrates that Eq. (6) adequately describes the fluctuation behavior of bilayer membranes under both positive and negative tensions.

From the fitting curves, one can extract the values of  $\kappa$  and  $\gamma \langle A_p \rangle$  as a function of  $\tau$ , and by independently measuring the mean projected area,  $\langle A_p \rangle$ , one can obtain the value of the fluctuation tension  $\gamma$ . Our attempts to use  $\kappa$  as a single fitting parameters by forcing  $\gamma = \tau$  resulted in poor fitting for negative tensions. The mean projected area as a function of  $\tau$  is plotted in the inset of Fig. 1. The observed increase in  $\langle A_p \rangle$  with  $\tau$  is anticipated and will be discussed in detail later. Figure 2 depicts the fluctuation tension  $\gamma$  as a function of  $\tau$ . The values reported in Fig. 2 are based on fitting analysis over the four longest fluctuation modes (smallest wavenumbers), and the error bars represent the intervals over which the fitting parameters,  $\gamma$  and  $\kappa$ , can be (mutually) varied while still producing reasonable fits up to the accuracy of the computational results. For non-negative tensions, our results agree very well with the relationship  $\tau = \gamma$ . As noted above in Sec. II, there is no reason for this equality to remain valid for negative tensions, and our analysis summarized in Fig. 2 reveals that, indeed,  $\gamma \neq \tau$  when the tensions are negative. Our results demonstrate that  $\gamma < \tau$  and, as also argued above, it is likely that the more rapid decrease in  $\gamma$  compared to  $\tau$  is related to the tendency of the membrane to form buckled configurations under negative tensions. The equality between  $\gamma$  and  $\tau$  is regained for  $\tau \approx -0.15$ , and then the trend changes, and  $\gamma$  becomes larger than  $\tau$ .

A closer inspection of the behavior of  $\gamma$  depicted in Fig. 2 reveals that the  $\gamma$  vs.  $\tau$  curve may be divided into three regimes: (i) a linear  $\gamma = \tau$  regime for  $\tau \geq 0$ , (ii) a non-linear regime where  $\gamma < \tau < 0$  for mildly negative frame tensions, and (iii) a plateau regime ( $\gamma \sim \text{const}$ ) for larger negative values of  $\tau$ . Saturation of the negative tension for strongly compress membranes was previously observed,<sup>22</sup> and we will return to the issue later in this section when we discuss our results for the physical area of the membranes (Fig. 4). The fluctuation

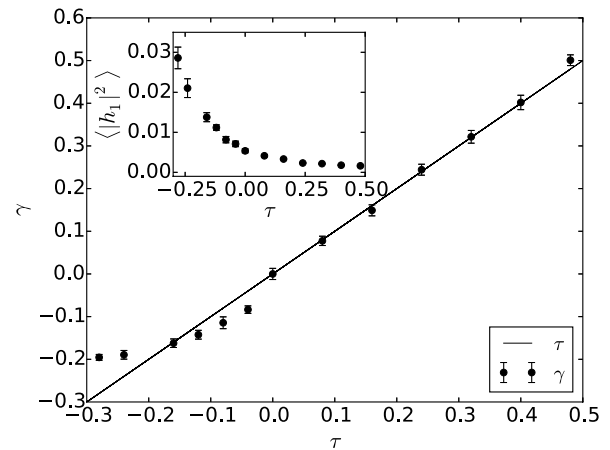


FIG. 2. The fluctuation tension  $\gamma$  as a function of the frame mechanical tension  $\tau$ . The solid line represents the equality  $\gamma = \tau$  which is expected to hold for positive tensions. The inset shows the spectral intensity of the longest Fourier mode ( $\vec{n}^2 = 1$ ),  $\langle |h_{\vec{1}}|^2 \rangle$ , as a function of  $\tau$ .

tension in Fig. 2 is extracted from Eq. (6), where it appears in the coefficient  $4\pi^2\gamma \langle A_p \rangle$  of the  $n^2$  term in the denominator. Naively, one may expect the saturation of the fluctuation tension  $\gamma$  to result in the leveling-off of the fluctuation spectral intensity  $|h_{\vec{n}}|^2$ . However, our computational results indicate that the amplitudes of the normal undulations continue to grow for decreasing values of  $\tau$ , as shown in the inset of Fig. 2. This apparent discrepancy can be only partially resolved by the trend in  $\langle A_p \rangle$  whose value is reduced by about 10% in the plateau regime of  $\gamma$ . The main factor explaining the increase in the undulation amplitude in the constant  $\gamma$  regime is the decrease in the effective bending modulus  $\kappa$ , the value of which is plotted in Fig. 3. We remind here that  $\kappa$  is not a material but a thermodynamic quantity. For a tensionless membrane, the thermal undulations reduce (renormalize) the bending rigidity by  $\Delta\kappa = -(3/4\pi)k_B T \ln(L/l)$ , which is a small correction.<sup>23</sup> For  $\tau < 0$ , the amplitude of the fluctuations increase and, therefore, this correction term should become larger (in absolute value), which explains the drop in the value of  $\kappa$  seen in Fig. 3. To state it in other words, just like the rapid decrease in  $\gamma$ , reported above in Fig. 2 for membranes under negative tension,

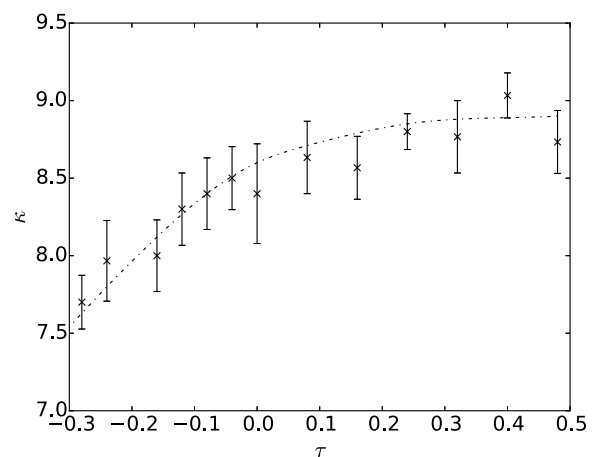


FIG. 3. The bending rigidity  $\kappa$  as a function of the frame tension  $\tau$ . The dotted-dashed line is a guide to the eye.

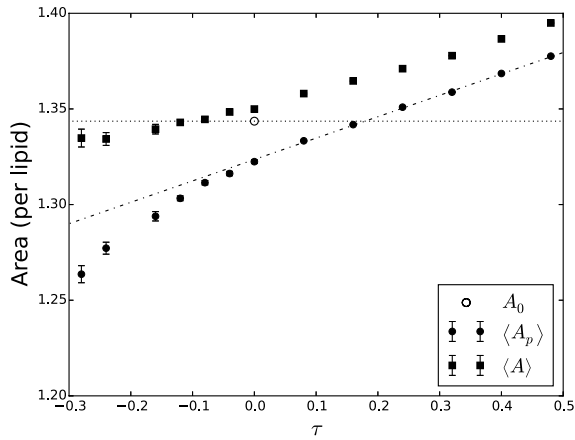


FIG. 4. Measured area as a function of the frame tension  $\tau$ . Solids circles and squares denote, respectively, the results for the frame and total areas. The former was measured directly from the simulation, while the latter was derived from the computed data for the spectral intensity, by using Eq. (7). The open circle marks the optimal area of a *flat* tensionless membrane,  $A_0$ . The dotted-dashed line is a linear fit for the results for  $\langle A_p \rangle$ , while the horizontal dotted line marks  $A_0$ . All areas plotted in the figure are normalized per lipid.

the reduction in  $\kappa$  is also related to the increasing thermal roughness of the membrane and the tendency of the membrane to form more buckled configurations.

The results of Figs. 2 and 3 point to an interesting difference between the elastic coefficients  $\gamma$  and  $\kappa$ . The former decreases faster than  $\tau$  for small negative tensions and levels-off at large negative tensions. The latter exhibits “opposite” behavior and remains fairly constant in the small negative tension regime, and then decreases for strongly compressed membranes. The crossover between the regimes occurs at  $\tau \simeq -0.15$ . Some light may be shed on these observations by the results of Fig. 4 depicting the mean projected and total areas as a function of  $\tau$ . The results for the mean projected area,  $\langle A_p \rangle$ , were measured directly from the simulations, while the data for the mean total area,  $\langle A \rangle$ , were calculated using Eq. (7). For  $\tau > 0$ , we observe a nearly linear dependence of both  $\langle A_p \rangle$  (see also the dotted-dashed line) and  $\langle A \rangle$  on  $\tau$ . This behavior agrees very well with the experimental results of Evans and Rawicz who also measured linear elastic response of giant unilamellar vesicles (GUVs) under positive mechanical tension.<sup>21</sup> We must point, however, to an important difference between the origins of linear elasticity in GUVs and small bilayer membranes. In both cases, the linear elastic response is energetic in nature and dominated by the area elasticity of the membrane, while the entropy and bending energy of the height fluctuations play a secondary role in the response to stretching. In GUVs, this happens after the height fluctuations have been ironed by a very weak positive tension scaling inversely with  $A_p$ . In small membranes, the height fluctuations are not damped and, in fact, the simulation results in Fig. 4 reveal that the excess area “stored” in the height fluctuations,  $\langle A \rangle - \langle A_p \rangle$ , decreases only weakly with  $\tau$ . This implies that the entropy and bending energy of small membranes do not vanish (as in GUVs under tension), but simply exhibit relatively weak dependence on the frame tension (and, therefore, contribute weakly to the elastic response).

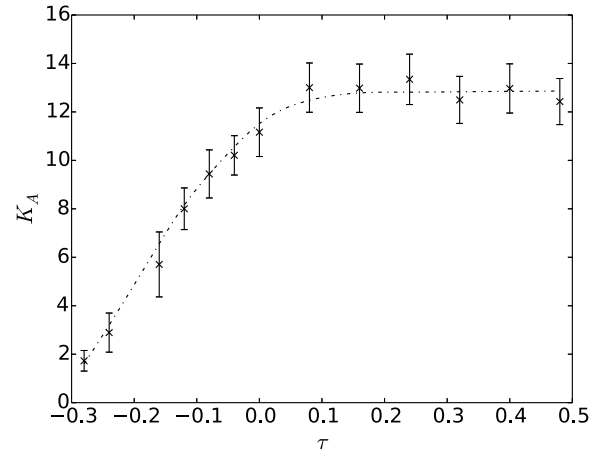


FIG. 5. The stretch modulus  $K_A$ , measured from Eq. (8), as a function of the frame tension  $\tau$ . The dotted-dashed line is a guide to the eye.

In addition to the simulations of fluctuating membranes, we also simulated a tensionless ( $\tau = 0$ ) *flat* membranes by running a MC code with moves allowing only local protrusions of lipids, but completely suppressing the longer scale bending modes (i.e., ensuring  $h_{\vec{r}i} = 0$  for all  $n$ ). For a flat membrane,  $A = A_p$ . The measured area of the flat tensionless membrane,  $A_0$ , is denoted by the open circle and the horizontal dotted line in Fig. 4. This is the area that minimizes the elastic energy of the membrane. Fig. 4 provides an interesting interpretation for the weak and strong negative tension regimes. The weak negative tension regime is essentially a continuation of the positive tension regime. The mean area of a tensionless fluctuating membrane is slightly larger than  $A_0$ , which implies that, in fact, the membrane is stretched despite the negative mechanical tension. Therefore, the area-dependent elastic energy continues to decrease with  $\tau$  into the weak negative tension regime. The strong negative tension regime begins when the total physical area reaches  $A_0$ . Since the membrane constitutes a dense fluid of lipids, it cannot be much further compressed, and in order to maintain the total area at  $A_0$ , more area must be expelled into the height fluctuations. At this point, the elastic response becomes dominated by the height fluctuations bending elasticity and entropy, and we begin to observe a reduction in the effective bending modulus,  $\kappa$ , instead of a reduction in the fluctuation tension  $\gamma$ . The saturation of the membrane physical area, and its correlation with that of the surface tension, was previously reported.<sup>22</sup> Here, we demonstrate that this occurs when  $\langle A \rangle$  reaches the value of  $A_0$ , which provided an intuitive explanation to these observations. Notice that the rapid decrease in the projected area  $\langle A_p \rangle$  with  $\tau$  in this regime is simultaneous to the increase in the projected area fluctuations. The resulting rapid decrease in the effective stretch modulus  $K_A$ , defined by Eq. (8), is plotted in Fig. 5. The vanishing of  $K_A$  signals the onset of mechanical instability.<sup>24</sup>

## V. DISCUSSION AND SUMMARY

Based on our results, we identify two negative tension regimes with the following features: (i) for weak negative tensions, the fluctuation tension  $\gamma$  drops somewhat faster than

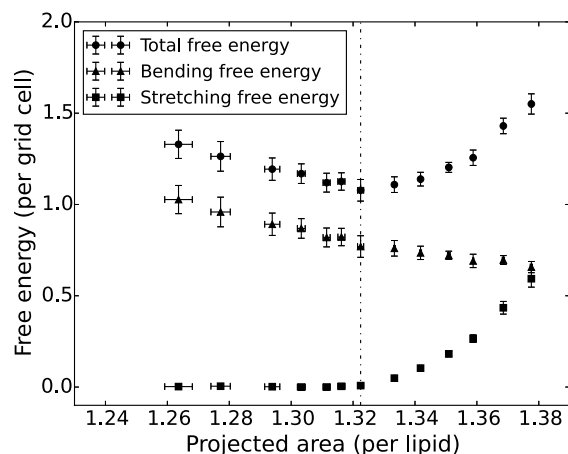


FIG. 6. The bending, stretching, and total free energies (see definitions in the text) per grid cell, as a function of mean projected area  $\langle A_p \rangle$  per lipid. The data for the total free energy have been shifted vertically by 0.3 for clarity. The vertical dotted-dashed line marks the measured projected area for  $\tau = 0$ .

the mechanical tension  $\tau$ , which is in contrast to the behavior observed for positive tensions where  $\gamma = \tau$ . In this regime, the membrane is still effectively stressed since the physical area  $\langle A \rangle > A_0$ . (ii) For strong negative tensions, the fluctuation tension saturates, but then the effective bending rigidity begins to fall. Additionally, we also find that the total membrane area in this regime reaches the optimal value of  $A_0$  and does not continue to drop much.<sup>25</sup>

In the spirit of Eq. (3) for the elastic free energy of positively stressed membranes, we can rationalize our observations for negatively stressed membranes by writing the free energy as the sum of two terms associated with stretching and bending. The former is given by the quadratic form  $F_{\text{stretch}} = (1/2) K_A [\langle A \rangle - A_0]^2 / A_0$ , while the latter may be evaluated by  $F_{\text{bend}} = (1/2) \kappa \sum_{\vec{n}} n^4 \langle |h_{\vec{n}}|^2 \rangle$ .<sup>26</sup> These two contributions and their sum are plotted in Fig. 6 as a function of  $\langle A_p \rangle$ . The free energies in Fig. 6 provide insight into the computational results in this work. First, we notice that the total free energy attains a minimum at  $\langle A_p \rangle / N \approx 1.32$  (marked by the vertical dotted-dashed line), which is the mean projected area measured for  $\tau = 0$ . This must be the case since  $\tau = \partial F / \partial A_p$ . Second, we notice that the bending free energy decreases with  $\tau$ , which is expected since, upon stretching, the thermal bending undulations tend to be suppressed. The stretching free energy increases with  $A_p$  in the weak negative and positive tensions regimes, i.e., when  $\langle A \rangle > A_0$ . Under strong negative tensions,  $F_{\text{stretch}}$  vanishes, which is associated with the observation that the total physical area remains at the optimal value and does not change in this regime.

The crossover from bending- to stretching-dominated membrane elasticity has also been observed in micropipette aspiration experiments of GUVs. There are, however, several key differences between the elastic behaviors of small and large membranes. Negative mechanical tension destabilizes the large bending modes of giant membranes, while small membranes can withstand a (size-dependent) negative tension that may be comparable in magnitude to the positive rupture

tension. In giant membranes, bending-dominated elasticity is limited to extremely small positive tensions that are typically two orders of magnitude smaller than the rupture tension. In small membranes, the crossover from bending-dominated to stretching-dominated elasticity is smoother and occurs at small negative tensions. In other words, the stretching-dominated elasticity regime extends into negative tensions, which stems from the fact that at zero tension, the membrane is still slightly stretched. Bending-dominated elasticity is observed at larger negative tensions. It is characterized by a decrease in the effective bending rigidity and stretch modulus of the membrane that ultimately leads to mechanical instability and membrane collapse.

## ACKNOWLEDGMENTS

This work was supported by the Israel Science Foundation, Grant No. 1087.13.

- <sup>1</sup>J. Israelachvili, *Intermolecular and Surface Forces* (Academic, London, 1985).
- <sup>2</sup>W. Helfrich, *Z. Naturforsch.* **28c**, 693 (1973).
- <sup>3</sup>U. Seifert and R. Lipowsky, in *Structure and Dynamics of Membranes*, edited by R. Lipowsky and E. Sackmann (Elsevier, Amsterdam, 1995), Chap. 8, pp. 403-463.
- <sup>4</sup>R. Lipowsky, in Ref. 3, Chap. 11, pp. 521-602.
- <sup>5</sup>R. Bruinsma and P. Pincus, *Curr. Opin. Solid State Mater. Sci.* **1**, 401 (1996).
- <sup>6</sup>P. Sens and S. Safran, *Europhys. Lett.* **43**, 95 (1998).
- <sup>7</sup>F. David and S. Leibler, *J. Phys. II* **1**, 959 (1991).
- <sup>8</sup>O. Farago and P. Pincus, *Eur. Phys. J.* **11**, 399 (2003).
- <sup>9</sup>J. H. Schulman and J. B. Montagne, *Ann. N. Y. Acad. Sci.* **92**, 366 (1961).
- <sup>10</sup>P. G. de Gennes and C. Taupin, *J. Phys. Chem.* **86**, 2294 (1982).
- <sup>11</sup>J. S. Rowlinson and B. Widom, *Molecular Theory of Capillary* (Clarendon Press, Oxford, 1982).
- <sup>12</sup>H. Diamant, *Phys. Rev. E* **84**, 061123 (2011).
- <sup>13</sup>Experimentally, the situation is more complicated since one deals with closed vesicles, whose projected area is not as well defined as the projected area of open bilayers with periodic boundary conditions. The thermodynamics of fluid vesicles was carefully analyzed in Ref. 12.
- <sup>14</sup>O. Farago and P. Pincus, *J. Chem. Phys.* **120**, 2934 (2004).
- <sup>15</sup>O. Farago, *Phys. Rev. E* **84**, 051914 (2011).
- <sup>16</sup>F. Schmid, *Europhys. Lett.* **95**, 28008 (2011).
- <sup>17</sup>I. R. Cooke, K. Kremer, and M. Deserno, *Phys. Rev. E* **72**, 011506 (2005). We slightly modified the model to avoid occasional escape of lipids from the bilayer.
- <sup>18</sup>Y. Y. Avital, N. Grønbech-Jensen, and O. Farago, *Eur. Phys. J. E* **37**, 69 (2014).
- <sup>19</sup>O. Farago and N. Grønbech-Jensen, *Biophys. J.* **92**, 3228 (2007).
- <sup>20</sup>O. Farago, *J. Chem. Phys.* **128**, 184105 (2008).
- <sup>21</sup>E. Evans and W. Rawicz, *Phys. Rev. Lett.* **64**, 2094 (1990).
- <sup>22</sup>W. K. den Otter, *J. Chem. Phys.* **123**, 214906 (2005).
- <sup>23</sup>K. Kleinert, *Phys. Lett.* **114**, 263 (1986).
- <sup>24</sup>It is worthwhile to re-emphasize the coupling between the statistics of the projected area and the height fluctuations, resulting from the saturation of the total area. Thus, the decrease in  $K_A$  does not reflect a change in the material stiffness of the bilayer membrane, but is simply just another reflection of the fact that it becomes increasingly buckled in response to  $\tau$  becoming more negative.
- <sup>25</sup>The determination of the physical area is based on Eq. (7), which is a Taylor expansion of  $\langle A \rangle$  for weakly fluctuating membranes. The slight decrease in  $\langle A \rangle$  observed for large negative tensions (i.e., when the membrane undulates more strongly) may be an artifact of this approximation.
- <sup>26</sup>The elastic free energy is obviously a function of the projected area  $F = F(A_p)$ . In the expressions here, the dependence on  $A_p$  is implicit through the dependence of the statistical averages of  $A$  and  $|h_{\vec{n}}|^2$  and through the values of the renormalized elastic moduli.